

Thermoelectric power and transport properties of $\text{Mg}_{1-x}\text{Al}_x\text{B}_2$

B. Lorenz,¹ R. L. Meng,¹ Y. Y. Xue,¹ and C. W. Chu^{1,2}

¹Texas Center for Superconductivity and Department of Physics, University of Houston, Houston, Texas 77204-5932

²Lawrence Berkeley National Laboratory, 1 Cyclotron Road, Berkeley, California 94720

(Received 2 April 2001; published 17 July 2001)

We have measured the thermoelectric power S and resistivity ρ of $\text{Mg}_{1-x}\text{Al}_x\text{B}_2$. S is positive and increases linearly with temperature above the superconducting transition temperature T_c . Deviations from the linear dependence appear at higher temperature, $T > T_0 \approx 160$ K. T_c and T_0 both decrease with Al doping whereas the slope of $S(T)$ in the linear range increases with the Al content. The data are discussed in terms of doping-induced changes of the Fermi surface and the density of states at the Fermi level.

DOI: 10.1103/PhysRevB.64.052513

PACS number(s): 74.25.Fy, 74.60.-w, 74.62.Dh, 74.70.Ad

The recent discovery¹ of superconductivity in MgB_2 at temperatures as high as 40 K has initiated a tremendous amount of experimental and theoretical activity with the goal of understanding the basic mechanism of superconductivity in this exciting compound. Two competing models^{2,3} were proposed to account for the superconducting properties in MgB_2 and the high T_c of 40 K. While both models attribute the superconductivity to the boron-sublattice conduction bands, the pairing mechanisms proposed differ significantly. Kortus *et al.*² suggested a BCS-type mechanism with strong electron-phonon coupling and high phonon energy of the light boron atoms. This mechanism is supported by the observation of an isotope effect on T_c ,⁴ a BCS-like superconducting gap structure,⁵ and a strong negative pressure coefficient of T_c .^{6,7} Alternatively, Hirsch and Marsiglio³ proposed a “universal” mechanism where superconductivity in MgB_2 is driven by the pairing of dressed holes. In fact, indications for hole-type conduction in the normal phase were found in the positive thermoelectric power.⁶ The hole character of carriers was confirmed recently by Hall measurements and the similarities to high- T_c superconductors have been discussed.⁸

Magnetic-susceptibility measurements on $\text{Mg}_{1-x}\text{Al}_x\text{B}_2$ have shown that electron doping suppresses T_c by a few degrees for up to 10% aluminum and superconductivity completely disappears due to a structural instability for $x > 0.1$.⁹ This negative doping effect on T_c could be explained by both pairing mechanisms discussed above. Within the BCS model the electron doping gives rise to an increase of the Fermi energy for electrons E_F , which is equivalent to a decrease of the Fermi energy for holes $E_{F\sigma}$, as referenced to the top of the hole-type σ band and a decrease of the hole carrier number. According to the band structure calculations of MgB_2 ,² the density of states $N(E_F)$ also decreases resulting in a lower T_c . In the “universal” mechanism,³ in analogy to high- T_c cuprates, the electron doping will reduce the number of hole carriers. In the underdoped regime T_c is also expected to decrease. However, for underdoped high- T_c compounds it is well known that the pressure coefficient of T_c is positive, contrary to the data for MgB_2 .^{6,7} Thermoelectric power S and resistivity ρ may give some insight into the normal-state conduction process and the electronic structure. We have, therefore, studied the temperature dependencies of

S and ρ of MgB_2 and the electron-doped solid solution $\text{Mg}_{1-x}\text{Al}_x\text{B}_2$ ($x < 0.1$). The data reveal a linear temperature dependence of S from T_c up to $T_0 \approx 160$ K, typical for the diffusion thermopower of metals. The positive sign and the low absolute value of several $\mu\text{V/K}$ are characteristic for a hole-type metallic conductor. However, the saturation of S close to room temperature shows that a more detailed consideration of the structure of the Fermi surface is needed to understand the transport properties. The slope of the linear part of $S(T)$ changes with Al doping and T_0 is reduced, indicating changes in the Fermi surface due to the electron doping.

Polycrystalline $\text{Mg}_{1-x}\text{Al}_x\text{B}_2$ samples were prepared by a solid-state reaction method as described earlier.^{6,9} X-ray powder-diffraction spectra of the samples show a minor amount of MgO as an impurity phase. The samples were dense enough to be connected with indium pads to thin platinum wires and thermocouples for resistivity and thermopower measurements, respectively. The resistivity was measured by the standard four-lead method using an ac resistance bridge LR 700. For thermoelectric power measurements we used a homemade apparatus and a sensitive ac technique with an accuracy of 0.1 to 0.2 $\mu\text{V/K}$. The room-temperature resistivity ρ increases from about 70 $\mu\Omega\text{ cm}$ to 120 $\mu\Omega\text{ cm}$ upon doping to 10% Al (Fig. 1). This increase is compatible with the reduction of hole carriers. However, the absolute value of ρ may strongly depend on porosity and grain-boundary scattering since the samples exhibit some porosity. The inset in Fig. 1 shows the resistivity close to T_c . All three samples ($x=0, 0.05, 0.1$) show a sharp resistance drop with a transition width < 0.5 K. The decrease of T_c by about 2 K for $x=0.1$ is in good agreement with the recent magnetization measurements.⁹ However, it should be noted that the undoped ($x=0$) sample shows a slightly lower T_c (38.5 K) than the highest so far reported value for MgB_2 . We attribute this difference to defects or deviations from stoichiometry reducing the T_c by about 1 K. The relatively low resistance ratio of our samples, $\rho(295\text{ K})/\rho(40\text{ K}) \approx 2$ to 3, as compared to values up to 20 reported for high purity MgB_2 wires and ceramics seems to reveal a large contribution from impurity scattering, particularly at a low temperature. In the present investigation we compare the effect of Al doping for samples prepared under identical conditions so

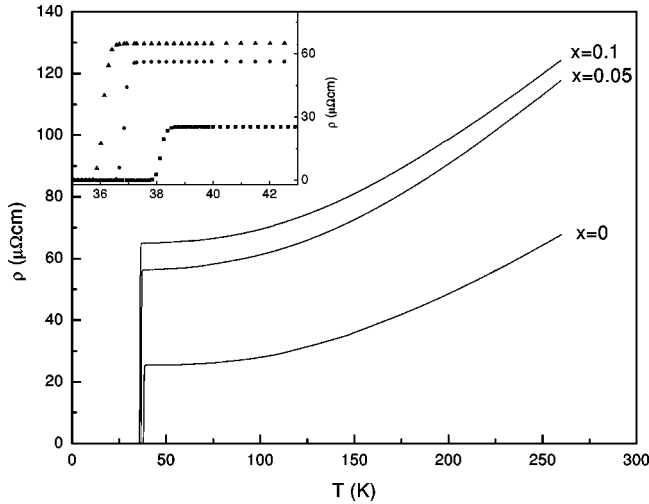


FIG. 1. Resistivity of $\text{Mg}_{1-x}\text{Al}_x\text{B}_2$. The inset shows the details near the superconducting transition.

that the shift of T_c can be considered as the relative change with respect to the undoped ($x=0$) material.

The temperature dependence of the thermoelectric power for $x=0, 0.05$, and 0.1 is shown in Fig. 2. The three curves are separated by an offset of $2 \mu\text{V}/\text{K}$ in order to better distinguish the data sets. The inset of Fig. 2 enlarges the superconducting transition region. The transitions are sharp

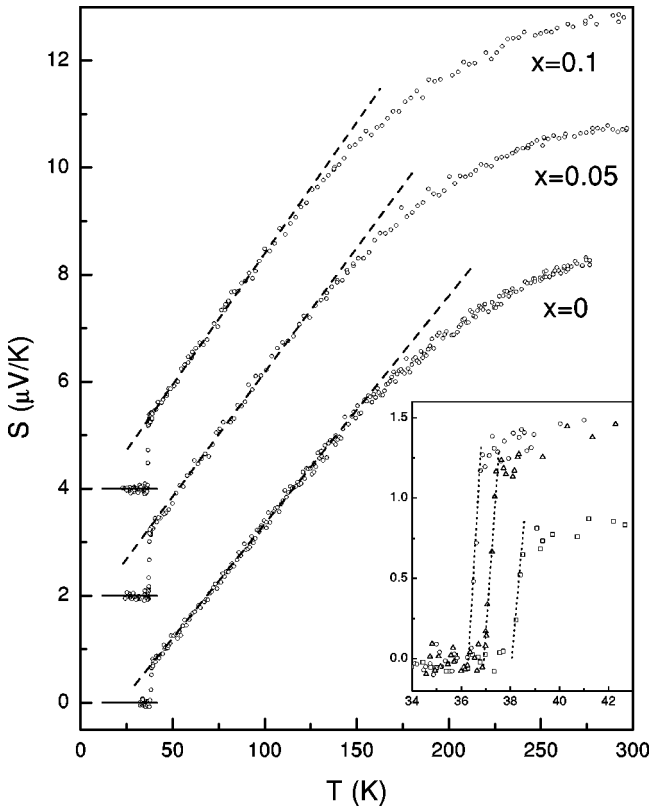


FIG. 2. Thermoelectric power of $\text{Mg}_{1-x}\text{Al}_x\text{B}_2$. For clarity, the curves are offset by a constant and the zero values are indicated by a short line. The inset shows the region of the superconducting transitions.

($<0.5\text{-K}$ width). The T_c decrease with increasing aluminum content x is consistent with the resistivity data and susceptibility experiments.⁹ Within the BCS theory the decrease of T_c with increasing electron number may be explained as a density of states (DOS) effect. The Fermi energy E_F is close to an edge of rapidly decreasing DOS and any increase of E_F due to Al doping will result in a remarkable decrease of $N(E_F)$. In the BCS description, T_c is given by the McMillan formula¹⁰

$$T_c \propto \omega \exp \left[\frac{-1.02(1+\lambda)}{\lambda(1-\mu^*)-\mu^*} \right], \quad (1)$$

where ω is the characteristic phonon frequency, μ^* the Coulomb repulsion, and $\lambda = N(E_F)\langle I^2 \rangle / M\langle \omega^2 \rangle$ is the electron-phonon coupling constant. $\langle I^2 \rangle$ is the averaged square of the electronic matrix element, M the atomic mass, and $\langle \omega^2 \rangle$ the averaged square of the phonon frequency. λ decreases proportional to $N(E_F)$, resulting in a decrease of T_c . It should be noted that Eq. (1) was also used successfully¹¹ to explain the observed decrease of T_c with external pressure.^{6,7}

The most interesting features of the thermoelectric power are the positive sign, the overall small value, and the linear dependence in the low-temperature range (indicated by dashed lines in Fig. 2). The positive but small value is typical for hole-type metals. This observation is supported by the results of band-structure calculations. Although the Fermi surface of MgB_2 shows a complex structure with sheets of hole-type as well as electron-type states,² it appears that the hole states dominate in the low-temperature ($T < T_0$) electronic transport. Recent Hall measurements also provide evidence for predominantly hole-type conduction in MgB_2 (Ref. 8) and extended band-structure calculations have shown that the positive Hall coefficient is the result of a superposition of positive and negative components in the polycrystalline sample.¹² Considering the linear $S \propto T$ dependence below 160 K, one is tempted to interpret the low-temperature part as the diffusion thermopower S_d of hole-type metals. In fact, according to the Mott formula the diffusion thermopower is linear in T if higher-order corrections are neglected,¹³

$$S_d = \frac{\pi^2 k^2 T}{3e} \left[\frac{\partial \ln \sigma(\epsilon)}{\partial \epsilon} \right]_{E_F}, \quad (2)$$

where k is Boltzmann's constant, e is the charge of the carriers, and $\sigma(\epsilon)$ is a conductivitylike function for electrons of energy ϵ . At low temperatures, in the residual resistance region, the carrier relaxation time is limited by impurity scattering and the logarithmic derivative in Eq. (2) is simply E_F^{-1} leading to the expression for S_d ,¹³

$$S_d = \frac{\pi^2 k^2 T}{3e E_F}. \quad (3)$$

Here E_F is the Fermi energy calculated from the edge of the conduction band. However, it is not expected that this simple formula is valid in the whole temperature range. First of all, in deriving Eq. (3) a spherical Fermi surface was assumed and a T -independent relaxation time was adapted. This approximation limits the application of Eq. (3) to low temperatures, i.e., the residual resistance region. Band-structure calculations show that the Fermi surface of MgB_2 is

far from being spherical and, in particular, also reflects the anisotropy of the layered structure.² Second, the deviation from linearity at T_0 and the saturation of S close to room temperature cannot be explained by Eq. (3). This phenomenon seems to be related to the complexity of the Fermi surface and the existence of electron-type sheets. These minor carriers may add a negative contribution to the Seebeck coefficient that increases at higher temperature. For the Al-doped samples the crossover temperature T_0 clearly decreases to about 130 K ($x=0.05$) and 118 K ($x=0.1$). However, for temperatures $T < T_0$ the experimental data perfectly follow the linear relation (3) and the temperature dependence of resistivity is small (indicating that impurity scattering is dominating). Assuming that electronic transport in this range is due to hole carriers in the σ bands we can use Eq. (3) to estimate the Fermi energy for these σ holes (for hole carriers this energy has to be referenced to the top of the σ bands). For MgB_2 the slope of $S(T)$ below 160 K is $0.042 \mu\text{V}/\text{K}^2$ and, according to Eq. (3), $E_{F\sigma} = 0.57 \text{ eV}$. This value is in fair agreement with the difference between the Fermi energy and the top of the σ bands of about 0.9 eV calculated by Suzuki *et al.*¹⁴ for MgB_2 . The smaller value for $E_{F\sigma}$ may be due to impurities or small deviations from stoichiometry reducing the number of holes from the theoretical value as discussed above. With increasing doping, the slope of $S(T)$ also increases to $0.047 \mu\text{V}/\text{K}^2$ ($x=0.05$) and $0.050 \mu\text{V}/\text{K}^2$ ($x=0.1$) indicating a decrease of $E_{F\sigma}$ by about 16% ($x=0.1$). This decrease is in very good quantitative agreement with the calculated 17% for $\text{Mg}_{0.9}\text{Al}_{0.1}\text{B}_2$.¹⁴ The results of this paragraph show that despite the complex structure of the Fermi surface, the transport properties of $\text{Mg}_{1-x}\text{Al}_x\text{B}_2$ in the low-temperature range are more similar to a conventional hole-type metal.

It is interesting to note that there is obviously no phonon drag contribution to the thermoelectric power of $\text{Mg}_{1-x}\text{Al}_x\text{B}_2$ (Fig. 2). The phonon drag effect is most common for pure metals and results in an enhancement of S in the low-temperature region. The absence of this contribution in MgB_2 has yet to be explained. The predominantly linear temperature dependence of $S(T)$ is similar to the thermopower of disordered metals where the phonon heat current is suppressed.¹³ Disorder could be introduced by high porosity, defects, impurities, or the dopant (Al) itself. In spite of the fact that the linearity $S \propto T$ is most pronounced in the pure MgB_2 where there is no Al on Mg sites, it is unlikely that the disorder induced by dopants may explain the absence of a phonon drag contribution to S .

We have not considered yet the possible anisotropy of the Seebeck coefficient. The thermoelectric tensor of hexagonal materials has two independent coefficients corresponding to

measurements made parallel (S_{\parallel}) and perpendicular (S_{\perp}) to the hexagonal axis. Both coefficients can be quite different, as shown for some hexagonal metals.¹⁵ Data from polycrystalline samples can only be considered as an average over all possible grain orientations. For example, S_{\parallel} and S_{\perp} of Zn are both nonlinear and of very different values over a large temperature range $0 < T < 300 \text{ K}$. Discussions of the Hall coefficients indicate a strong anisotropy in different crystallographic directions.¹² From the shape of the MgB_2 Fermi surface it could be expected that the Seebeck coefficient is anisotropic. Note that the hole-type areas form cylinders (bonding $p_{x,y}$ bands) running along Γ -A- Γ and a perpendicular tubular network (bonding p_z bands) whereas the electron-type sheets form only a tubular network in the plane perpendicular to Γ -A- Γ (antibonding p_z bands).² This anisotropy should be more obvious at higher temperature where the scattering is determined by phonons. In the low-temperature impurity scattering range and in the absence of the phonon drag contribution the Seebeck coefficient is expected to show less anisotropy. In the lack of MgB_2 single crystals it appears difficult to measure the anisotropy of the thermopower. However, c -axis oriented thin films of MgB_2 may be used to extract the in-plane Seebeck coefficient S_{\perp} .

In conclusion, the resistivity and thermoelectric power of polycrystalline $\text{Mg}_{1-x}\text{Al}_x\text{B}_2$ have been measured. The decrease of T_c with Al doping previously deduced from susceptibility measurements was confirmed. The Seebeck coefficient of undoped MgB_2 was found to increase linearly with temperature from T_c to about 160 K. This increase, the positive sign, and the overall small value of S are compatible with the assumption that $\text{Mg}_{1-x}\text{Al}_x\text{B}_2$ is a hole-type normal metal. This result is further supported by the increase of the slope of $S(T)$ with electron doping. Deviations from linearity at higher temperatures are discussed in terms of a contribution from electronlike sheets of the Fermi surface. The origin of the missing phonon drag contribution is still an open question. The Seebeck coefficient of MgB_2 may be anisotropic and measurements of single crystals or oriented thin films are required. The current data yield indirect support of the BCS mechanism for the superconducting transition.

This work was supported in part by NSF Grant No. DMR-9804325, MRSEC/NSF Grant No. DMR-9632667, the T. L. Temple Foundation, the John and Rebecca Moores Endowment, the State of Texas through the Texas Center for Superconductivity at the University of Houston, and the Lawrence Berkeley Laboratory by the Director, Office of Energy Research, Office of Basic Sciences, Division of Material Sciences of the U. S. Department of Energy under Contract No. DE-AC0376SF00098.

¹J. Nagamatsu, N. Nakagawa, T. Muranaka, Y. Zenitani, and J. Akimitsu, *Nature (London)* **410**, 63 (2001).

²J. Kortus, I.I. Mazin, K.D. Belashchenko, V.P. Antropov, and L.L. Boyer, *Phys. Rev. Lett.* **86**, 4656 (2001).

³J.E. Hirsch, cond-mat/0102115 (unpublished); J.E. Hirsch, and F.

Marsiglio, cond-mat/0102479 (unpublished).

⁴S.L. Bud'ko, G. Lapertot, C. Petrovic, C.E. Cunningham, N. Anderson, and P.C. Canfield, *Phys. Rev. Lett.* **86**, 1877 (2001).

⁵G. Rubio-Bollinger, H. Suderow, and S. Vieira, cond-mat/0102242 (unpublished); G. Karapetrov, M. Iavarone,

- W.K. Kwok, G.W. Crabtree, and D.G. Hinks, Phys. Rev. Lett. **86**, 4374 (2001); A. Sharoni, I. Felner, and O. Millo, cond-mat/0102325 (unpublished); H. Kotegawa, K. Ishida, Y. Kitaoka, T. Muranaka, and J. Akimitsu, cond-mat/0102334 (unpublished).
- ⁶B. Lorenz, R.L. Meng, and C.W. Chu, Phys. Rev. B **64**, 012507 (2001).
- ⁷E. Saito, T. Taknenobu, T. Ito, Y. Iwasa, K. Prassides, and T. Arima, J. Phys.: Condens. Matter **13**, L267 (2001).
- ⁸W.N. Kang, C.U. Jung, K.H.P. Kim, M. Park, S.Y. Lee, H. Kim, E. Choi, K.H. Kim, M. Kim, and S. Lee, cond-mat/0102313 (unpublished).
- ⁹J.S. Slusky, N. Rogado, K.A. Regan, M.A. Hayward, P. Khalifah, T. He, K. Inumaru, S. Loureiro, M.K. Haas, H.W. Zandbergen, and R.J. Cava, Nature (London) **410**, 343 (2001).
- ¹⁰W.L. McMillan, Phys. Rev. B **167**, 331 (1968).
- ¹¹I. Loa and K. Syassen, Solid State Commun. **118**, 279 (2001).
- ¹²G. Satta, G. Profeta, F. Bernardini, A. Continenza, and S. Massidda, cond-mat/0102358(unpublished).
- ¹³F. J. Blatt, P. A. Schroeder, and C. L. Foiles, *Thermoelectric Power of Metals* (Plenum Press, New York, 1976).
- ¹⁴S. Suzuki, S. Higai, and K. Nakao, cond-mat/0102484 (unpublished).
- ¹⁵V.A. Rowe and P.A. Schroeder, J. Phys. Chem. Solids **31**, 1 (1970).